STUDY OF CO-EXISTENCE OF SUPERCONDUCTIVITY AND FERROMAGNETISM IN Pr DOPED $YBa_2Cu_3O_{7-\delta}$

A THESIS SUBMITTED TO
THE SCHOOL OF GRADUATE STUDIES OF
ADDIS ABABA UNIVERSITY

IN PARTIAL FULFILLMENT OF THE
REQUIREMENTS FOR THE DEGREE OF
MASTER OF SCIENCE IN PHYSICS

By

Moges Tsega

ADDIS ABABA, ETHIOPIA
JULY 2005

Acknowledgements

I would like to thank Professor P. Singh, my advisor, for help with ideas and interpretations and who with great patience has helped me write comprehensible thesis, and always finds time for discussion. His constant enthusiasm for physics has been an excitement and an encouragement that help me make rapid progress during the research.

I take pleasure to convey my warmest thanks to my friend Melkie Admassie, for his non-volatile support and encouragement both morally and financially. I feel it a matter of lifelong indebtedness towards my parents for their love, affection, and they are truly steep stones for my success.

I feel immense pleasure to express my deep sense of gratitude to my wife Hanna George for waiting nights, her support and encouragment and giving me other sides of life than physics. Finally, Heartfelt thanks to my friends for their encouragement.

Abstract

The co-existence of superconductive and magnetic properties of $Y_{1-x}Pr_xBa_2Cu_3O_{7-\delta}$ has been investigated. The suppression of T_c by the Pr concentration can be described by the Abrikosov-Gorkov pair-breaking like relation, and hybridization between Pr 4f states and conduction bands may play an important role in the suppression of T_c. We have determined the dependency of T_c on the impurity concentration. Superconductivity vanishes at a certain critical concentration. We have made a detailed study of co-existence of superconductivity and ferromagnetism in the concentration range close to the critical. We also study the effect of spin-spin interaction at $T < T_m$ and spin-electron interactions on superconducting transition point. Superconductivity appears together with ferromagnetism but persists only until the ferromagnetic effect is not sufficiently large.

Table of Contents

Introduction

Superconducting materials are finding increasing use in the generation of high magnetic fields, in loss-less electrical power transmission and storage, in magnetic sensors, in electromagnetic radiation detectors and in high speed digital signal and data processing. Since the discovery of superconducting materials with T_C above the boiling point of liquid nitrogen (77K), these materials are roughly divided into two categories, viz., low and high T_C superconductors. Superconductivity which is the state of zero resistance, was first discovered by H. Kamerlingh Onnes [1]. He also discovered that superconductivity was destroyed by the application of a sufficiently strong magnetic field or on the passage of sufficiently strong electrical current. The transition from superconducting to normal state can be sharp (Type I superconductors) or broad (Type II superconductors). Most of the practical materials are type II. In these materials microstructure plays an important role. The theory of type II superconductivity was given by Ginsburg, Landau, Abrikosov and Gorkov and is usually called GLAG theory. These researchers showed that the type I or type II behavior is determined by the ratio $\kappa = \lambda_L/\xi$ where λ_L is the London penetration depth and ξ is the coherence length.

Typically, this ratio, κ, is less than $\frac{1}{\sqrt{2}}$ for type I, and greater than $\frac{1}{\sqrt{2}}$ for type II superconductors. In low temperature superconductors their transition temperature below 30K are called conventional superconductors, and explained by BCS theory of electron-phonon interaction. Elements, like Pb (T_c=7.2 k), Sn (T_c=3.7K), and alloys like Nb_3Sn ($T_c = 18\ k$) are grouped under this category. On the other hand, many of Ce, U and Yb compounds, which have localized f electrons, and are generally called heavy fermion systems. One of the most attractive feature of this system is the appearance of superconductivity in a few U-based and Ce-based compounds. Since non-magnetic impurity scattering suppresses an anisotropic cooper pair wave function, it has been interpreted as evidence for unconventional non s-wave pairing [2]. Heavy fermion materials show competition, co-existence, and /or coupling of magnetic and superconducting order parameter like in $CeCu_2Si_2$ [3].

High -T_c superconductors, exhibit the main superconducting properties including zero-resistance, Meissner effect, flux quantization, Josephson effects, and gaps in the excitation energy spectrum, and also characterized by a two-dimensional structure, a short coherence length ξ and two energy gaps. The magnetic field penetrates the material slowly at a value denoted by H_{c1} and continues up to a value denoted by H_{c2} at which point the material is transformed to normal (non-superconducting) state. The superconducting state between H_{c1} and H_{c2} is called mixed state. Under this category compounds of organic, and cuprates are included. Cuprate superconductors are oxide superconductors with perovskite structure.

In 1986 Bednorz and Muller [4] observed evidence of superconductivity with transition temperature over 30K in $La_{2-x}Ba_xCuO_4$. This material had perovskite structure. A substitution of Yttrium for Lanthanum led to the discovery of $YBa_2Cu_3O_{7-\delta}$ often referred to as YBCO or 123 because of the ratio of Y:Ba:Cu in this material. This was the first superconductor discovered with a T_c in the range 90-95K, [5] well above the boiling point of liquid nitrogen. This discovery was followed in 1988 by the discovery of Bismuth ($Bi_2Sr_2Ca_2Cu_3O_{10+\delta}$) and Thallium ($Tl_2Ba_2Ca_2Cu_3O_{10+\delta}$) based superconductors with even higher T_c. So we have an ever increasing T_c superconductivity in the recent years and the search for room temperature superconductivity is vigorously on. Superconductivity over the years is shown in Fig. 1.

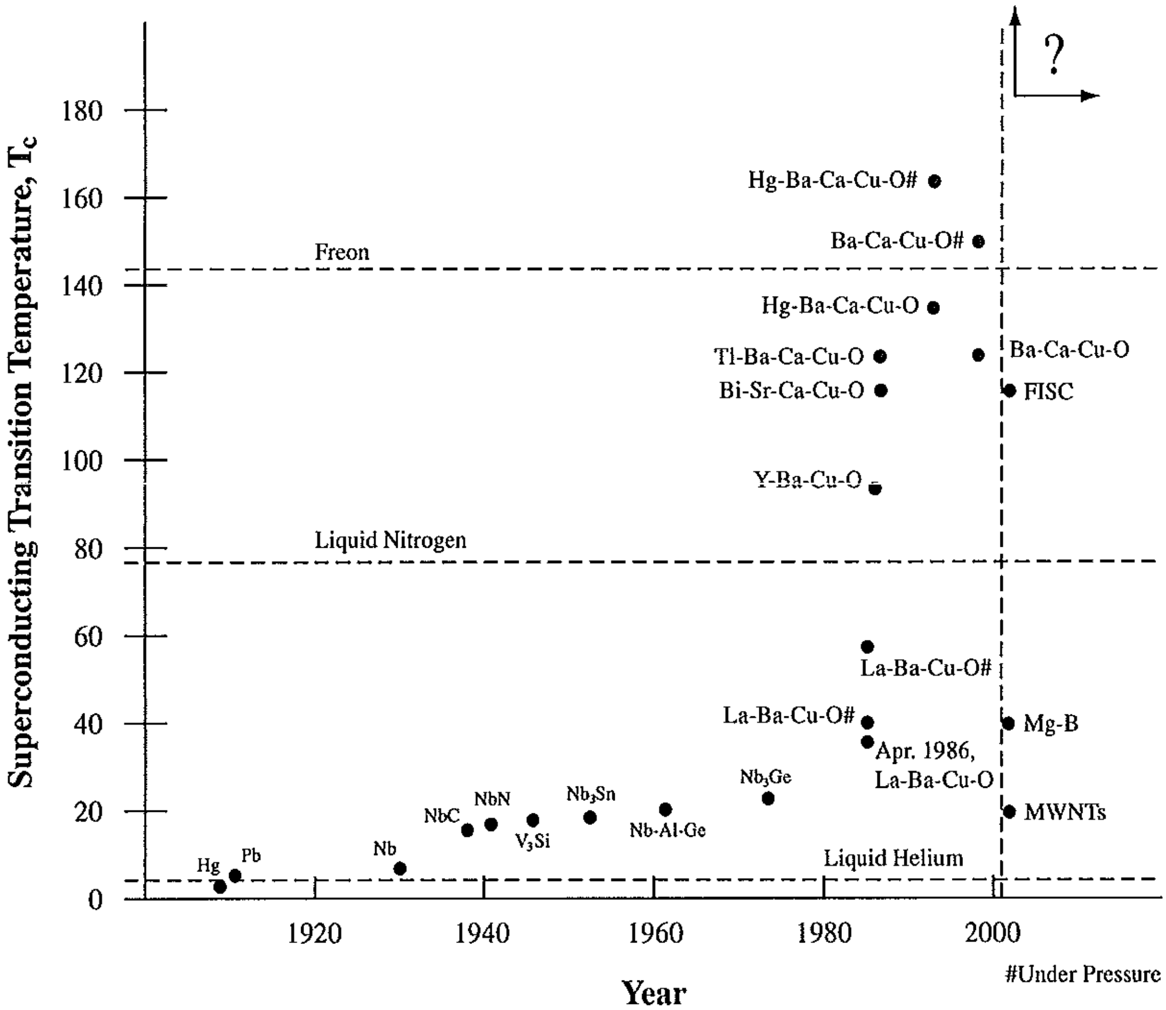

Figure 1: Superconductivity through the years.

Chapter 1

REVIEW LITERATURE

There are a number of theories related to high temperature superconductors that have been put forward to understand the pairing mechanisms in high T_c superconductors. After the discovery of high T_c superconductor La (Ba/Sr)CuO at 37K [4] most of the workers believed that conventional BCS theory is not adequate to explain the superconductivity with such high transition temperatures. Although there have been much studies on the impurity doping effects in high T_c superconductors, it has not been successful to understand the underlying physics. In particular, the decrease of T_c due to impurity scattering is not fast enough to support the anisotropic pairing such as d-wave or anisotropic s-wave pairing. In conventional low T_c superconductors, it was shown that the AG (Abrikosov-Gorkove) Green function theory is in conflict with the Anderson [6] theory of dirty superconductors predicted as no T_c decrease with ordinary impurity substitution in contrary to AG's theory [7]. Therefore, the mechanisms of T_c suppression in $Y_{1-x}Pr_xBa_2Cu_3O_{7-\delta}$, and magnetic ordering when magnetic impurity is added to the YBCO system is also matter of debate. In the present chapter, we have reviewed the theoretical formulation and experimental work, which are closely related to our investigation.

1.1 Basic Elements Of BCS Theory

When electrons move through a substance, collisions occur with thermally displaced ions and impurities or defects, which lead to resistance. Obviously superconductors did not suffer from this effect, and this phenomena is explained properly by the BCS theory [8], specially for low temperature superconductors. The central feature of this theory is that two electrons in the superconductors are able to form a bound state called a cooper pair if they somehow experience an attractive interaction. The lattice structure is momentarily deformed by the passing electron, and also known as electron-phonon interaction. If an electron is pushed through the lattice structure of the superconductor, the positively charged ions will be attracted to this localized negative charge. As the electron is moving, by the time the ions have moved to where the electron was, an excess localized positive charge is created. This attracts another nearby electron (the second electron in the cooper pair) as shown in Fig.1.1. If there are no imperfections to scatter, the electrons form Cooper pairs which move with out any resistance and loss of energy. A Cooper pair consists of two electrons with equal and opposite spin and momenta, and has zero spin and momentum. So any applied magnetic field would increase the energy of one electron, while decreasing the energy of the other by the same amount. This would have a zero net benefit to the pair. If the magnetic field is strong enough, the electrons may split up, and therefore remove the superconducting ability.

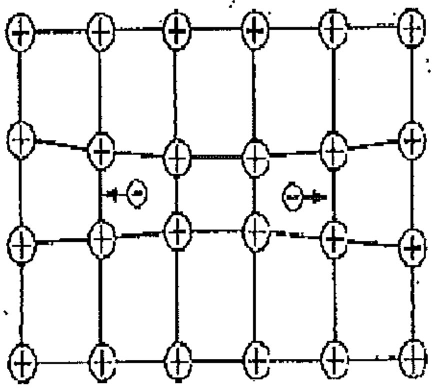

Figure 1.1: Basic Visualization of the phonon-electron interaction.

1.1.1 Cooper Pairing

The cardinal process behind superconductivity is the formation of Cooper pairs. Cooper, who originally studied the problem [8], showed that fermions, interacting above a closed Fermi sea, will show an instability towards forming pairs regardless of the weakness of the interaction, so long as the interaction remains attractive. Due to the sharpness of the Fermi surface, the main contribution to this population of paired states will arise between atoms on opposite ends of the Fermi surface. For instance we consider the s-wave paring of a two spin state system $(\uparrow, \downarrow)$, pairs will prefer to form between atoms of $\mathbf{k}, \uparrow$ *and* $-\mathrm{k}, \downarrow$ (see Fig. 1.2). In a true many-body system, these atom pairs do not truly form bound states, but should rather be thought of as resulting from strong correlations. The energy gap, and most of the observed properties of superconductors, would be absent if it weren't for the strong correlations between these pairs. It should be noted, however, that these correlations result more from the Pauli blocking of available states within the Fermi surface than from the actual dynamical interactions.

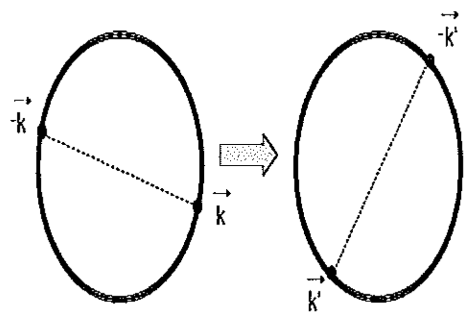

Figure 1.2: Diagram illustrating the formation of Cooper pairs.

As a consequence, it is often a very good approximation to treat the system as though the interactions only occur between the Cooper pairs. This scheme may be called the BCS or pair approximation.

1.1.2 Meissner effect

It was discovered in 1933 by Meissner and Ochsenfeld [9] that a superconductor will expel a weak magnetic flux from its interior, and hence acting like a perfect diamagnet. If the field gets too large, however the material will eventually lose its superconducting state.

1.1.3 Isotope effect

The critical temperature of a superconductor is a property of mass of the atomic nucleus of the lattice ions. One validation of this idea is the isotope effect. It can be shown that T_c of the superconductor is inversely proportional to the mass of the positive ions especially for phonon mediated superconductivity. Since neutrons carry no charge, they do not affect the Coulombic interactions between electrons and lattice ions, but they do change the rates at which phonons can propagate through the lattice. A phonon is a mechanical wave, and it is one of the fundamental ingredient of the BCS theory. Experimentally, it was found that M^{α} T_c= constant, where α is the isotope effect constant.

1.1.4 Thermodynamic properties

There are several thermodynamic changes that occur in a superconductor as it makes its transition from the normal state ($T > T_c$) to the superconducting state ($T < T_c$). The existence of an energy gap, or energy interval with no allowed eigen energies in the energy spectrum, i.e., there is an energy gap, only an exponentially small number of particles having enough thermal energy be promoted to the available unoccupied states above the gap. The specific heat capacity of an electron changes from linear to an exponentially relationship, and include in this change is a second-order phase transition that increases the specific heat many times as temperature is decreased to below ($T < T_c$).

1.2 Pairing Mechanisms in high T_c Superconductors

The discovery of high-temperature superconductors has been an intensive search, for understanding the essential mechanism of superconductivity. It has become clear that the superconducting transition temperatures are too high to be explained by the theory based on vibrations of the atoms. In fact the pairing mechanism is well understood in low temperature superconductivity. Bardeen, Cooper and Schriefer [8] gave the the first remarkable theory based on pairing of charge carriers through electron lattice interaction to understand the phenomenon of superconductivity. They derived an expression for T_c and explained experimental results of conventional superconductors. The superconductivity of Fullerence compounds Potassium, Rubidium and Cesium carbon-60 has also been studied. It was observed that when 13C atoms were substituted for 12C atoms in buckyball molecules, T_c of the RbC_{60} sample decreased by an amount one would expect from BCS theory, which describes superconductivity in terms of electron pairs mediated by phonons [10]. On the other hand, Chakravarty et al. [11] proposed that there may be an effective interaction between electrons for a C_{60} molecule of a purely electronic mechanism. The attractive interaction has been evaluated on the basis of the Hubbard model for a single C_{60} molecule and the possibility of singlet superconductivity that depends on the effective intra-ball electron-electron repulsion and the inter-ball hopping amplitude.

In heavy fermion superconductivity, there is an idea that the superconductivity paring is mediated by magnetic interactions. This has been suggested from the pressure induced superconductivity in $CeIn_3$, and $CePd_2Si_2$, which occurs with suppression of magnetism with increasing pressure by enhancing hybridization between conduction electrons and local moments [12]. On the other hand, after the discovery of unconventional property in UPt_3 superconductor, it was realized that the occurrence of superconductivity instability in the heavy-electron liquid gave rise to speculations about an unconventional electron-electron pairing mechanism and an unusual symmetry of the Cooper pairs [13].

In the conventional superconductors the phonon mediated electron Cooper pairing is evidenced by the presence of isotope effect in the system. But the near absence or marginality of isotope effect especially in Y-Ba-Cu-O is puzzling both experimentalists and theorists alike, and they proposed different mechanisms for high T_c superconductors. Ching et al. [14] have explained high temperature superconductivity in $YBa_2Cu_3O_{7-\delta}$ system using excitonic enhanced superconductivity mechanism.

Experiments by Bourne et al. [15] suggest that the absence of oxygen isotope effect shift in high temperature superconductors $YBa_2Cu_3O_{7-\delta}$ through substitution of ^{18}O for ^{16}O shows that a non-phonon mechanism may be important in this material. As electronic and magnetic excitations are at energies higher than the phonons, they can lead to higher transition temperature and are considered as an alternative mechanism of pairing.

Verma et al. [16] suggested a purely electronic pairing mechanism for superconductivity which is specific to the electronic structure of the oxide superconductors. They argued that newly discovered high T_c oxide metals have a low enough electron density that the charge transfer excitations between nearest neighbors cations and anions are unscreened. Excitonic resonances with a large oscillator strengths are then possible. It was further suggested that the high T_c is due to scattering of electrons from such resonances rather than phonons.

Singh and Sinha [17] have proposed a mechanism which involve the role of electron pair in single state species $X^{\uparrow\downarrow}$ such as Cu^{+1}, O_2^{2-} and their virtual excited state X^0 such as Cu^{3+}, O_2^0 in pairing interaction of quasiholes. They have applied this theory for $YBa_2Cu_3O_{7-\delta}$ and explained the variation of T_c with hole concentration. Singh and Sinha [18] also proposed a new mechanism for high temperature superconductors (HTSC) involving bi-excitons. Bi-excitons result from the possible electronic polarization of surrounding medium in which two layers are embedded correlated charge transfer from complex $O^- - Cu^+ - O^-$ to complex $O^{2-} - Cu^{3+} - O^{2-}$ is considered. It is argued that this process may take precedence over the correlated charge transfer pair only when energies are nearly degenerate. They have proposed that it is capable to explain the entire possible range of high T_c. Generally to say, even though a number of theories has been proposed to explain the normal state and superconducting properties of HTSC, there is no agreement as to which model is appropriate. The only consensus on the electronic properties of the normal state of HTSC is that they are not conventional and perhaps non-phonon mediated. Spin glass ordering in Y-based superconductors containing Fe has also been studied by Singh and Kishore [19], and by Singh and Singh [20].

1.3 Overview of the Properties of $YBa_2Cu_3O_{7-\delta}$

The superconducting phase in all the cuprates has common features. They are all type II superconductivity. Most of the high temperature materials are layered cuprates i.e., they consist of CuO_2 planes separated by layers of other elements or oxides. Because high temperature materials exhibit strong anisotropy i.e., the values of superconducting parameters are different in different directions. In addition, charge transport is mainly confined to the CuO_2 planes. YBCO is one of the most actively studied high temperature materials, and has numerous advantages as compared to the other ceramic superconductors by

- The only known stable four-element compound with $T_c > 77$K.
- It includes neither toxic elements nor volatile compounds.
- Easy to make single-phase YBCO.
- Less anisotropic than other high temperature materials, carries higher current densities at higher magnetic fields. Experimentally, the critical temperature of YBCO is approximately 92K and the critical magnetic field can be as high as 300T. For thin film applications, Critical density (J_c) is an important parameter, and typically $J_c \geq 1MA/(cm)^2$. The dimensions of a single unit cell are $a = 0.382nm$, $b = 0.389nm$, and $c = 0.1168nm$. The lattice is composed of so-called Perovskite layers (ACuO_3), where A represents a rare-earth or an alkaline-earth element (e.g., Yitrium or Barium in YBCO respectively). The term $7 - \delta$ in the chemical formula implies a slightly deficiency of oxygen. When δ =0, the CuO-chains are perfectly ordered and the lattice is in the orthorhombic phase ($a \neq b \neq c, \alpha = \beta = \gamma = 90^0$). When δ =1 YBCO has a

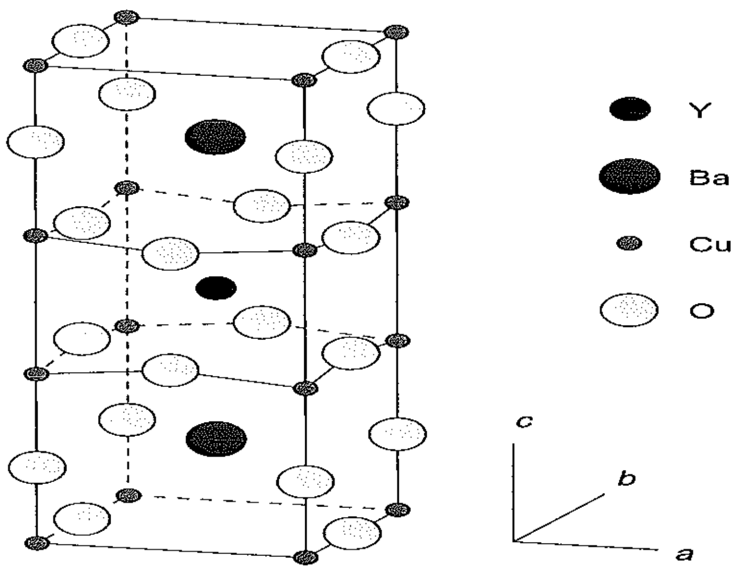

Figure 1.3: The unit cell structure for $YBa_2Cu_3O_{7-\delta}$.

tetragonal structure ($a = b \neq c, \alpha = \beta = \gamma = 90^0$). Only the orthorhombic structure is superconducting, which is the host compound for our interest, but unfortunately it is stable only at temperature below 500^0C.

The superconductivity in YBCO material is anisotropic, and the penetration depth of a field applied parallel to the CuO_2 planes can be up to many times larger then the penetration depth of a field applied normal to the planes. This is normally regarded as evidence that conduction is predominantly due to the motion of carriers in the CuO_2 planes. The high T_c and small fermi velocity of $YBa_2Cu_3O_{7-\delta}$ means that the coherence length, which measures the size of cooper-pair wave functions, is comparable to the size of the unit cell. In contrast, the low carrier density implies that the penetration depth is large, and the superconductivity is referred as type II with very large value of H_{c2}. Generally, type II superconductors have two critical fields: the lower and the upper critical fields (H_{c1} and H_{c2},respectively). If the applied field $H < H_{c1}$, the material is in the superconducting Messiner state. When the external magnetic field is between the two critical values, the material is in the mixed state shown in Fig. 1.4, and above H_{c2} the superconductivity of type II disappears completely [21]. On the other hand the critical temperature increases with the doping up to some point known as the optimal doping point, increasing the doping further results a reduction in T_c. The doping regimes below and above the optimal doping are known as the underdoped and overdoped regimes, respectively shown in Fig. 1.5. Even though a complete understanding of the properties of $YBa_2Cu_3O_{7-\delta}$ can only be obtained by taking into account its three-dimensional structure, the discussion of its behavior is simplified by regarding each CuO_2 plane as an isolated two-dimensional systems. Thus, we can summarize the general properties of YBCO using typical superconducting parameters having corresponding values which is given experimentally.

Critical temperature	$T_c = 90 - 92K$ [22]
Critical magnetic fields	H_{c1}=10mT, H_{c2}=300T [21]
London penetration depths	λ_{ab}=10nm, λ_c=200nm [21]
Coherence lengths	ξ_{ab}=3nm, ξ_c=0.4nm [21]

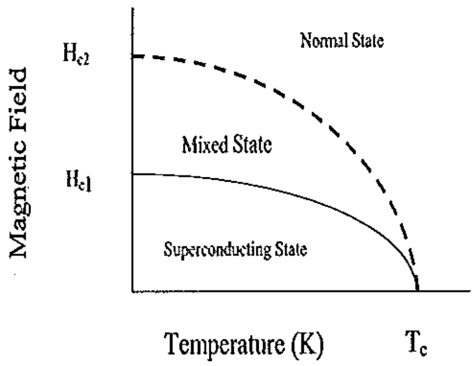

Figure 1.4: Phase diagram for the critical magnetic fields in cuprates.

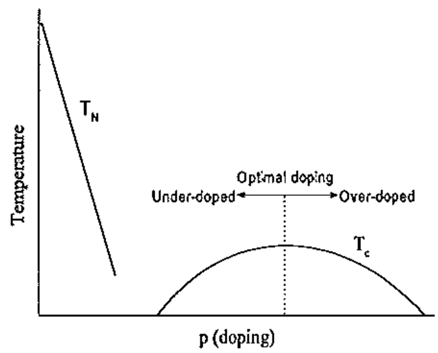

Figure 1.5: The main feature of the phase diagram for the doped cuprates.

1.4 Magnetism and Superconductivity in $Y_{1-x}Pr_xBa_2Cu_3O_{7-\delta}$

The interplay between magnetism and superconductivity is inherently of great interest since two phenomena represent ordered states which are mutually exclusive in most systems, and it is well established that the high T_c superconductors are antiferromagnetic ordering in the normal state. It means, there is some relation between superconductivity and magnetism. In an effort to understand the unique superconducting pair-breaking properties of Pr substituted YBCO, we have undertaken a study of superconducting and magnetic properties of $Y_{1-x}Pr_xBa_2Cu_3O_{7-\delta}$, spanning the complete composition range $0 \leq x \leq 1.0$ from a 92K superconductor (x=0) to high-resistivity semiconductor with antiferromagnetism (x=1.0). Kebede et al. [23] study reveals a smooth evolution $Y_{1-x}Pr_xBa_2Cu_3O_{7-\delta}$ from superconductivity ($x < 0.6$) to antiferromagnetic ordering ($0.4 < x < 1.0$), and suggest a magnetic order-superconductivity overlap region for $0.4 < x < 0.6$. They [23] experimentally verified that, T_c decreases and magnetic ordering transition temperature rises monotonically as x increases and a possible overlap between in the region, $0.4 < x < 0.6$, where magnetism and superconductivity possibly co-exist.

1.4.1 Effect of Doping of Pr on $YBa_2Cu_3O_{7-\delta}$

Praseodymium (Pr) is a soft, silivery-yellow, malleable, dectile metal. More resistant in air than some other rare earths, it develops a green oxide coating that spalls off when exposed to air. Pr is never found free in nature, appearing only in combined form with other rare earths in various minerals, and its crystal structure is double C-axis hexagonal close packed (dhcp) produced by stacking sequence of ABAC. As we compared rare earth ions with the iron group, the crystal field would be weaker, because the 4f electrons are deeper in the ion, and the spin-orbit interactions would be stronger, because the magnetic electrons are nearer the nucleus. In the metallic state, the 4f electrons on a rare earth ion are subjected to a variety of interactions with their surroundings. These forces may be broadly classified into two categories. The single ion interactions act independently at each ionic site so that their influence on the state of 4f electrons at a particular site unaffected by the magnetic state of its neighbors. The corresponding contribution to the Hamiltonian therefore contains sums over terms located at the ionic sites, if the crystal, but with out any coupling between different ions. On the other hand, the two-ion interactions couple the 4f-clouds at pair of ions, giving terms which involve two sites i and j. Pr doping is still probably one of the most controversial issues regarding YBCO.

The most specular observation of course is superconductivity in Pr-123 as first suggested by Blacktsead et al. [24] who observed a small decrease in the surface resistance at 92K and the recent observation by Zou et al. [25] of bulk superconductivity in some parts of a Pr-123 sample. One reason for the large interest in the area is the hope of finding the mechanism giving high temperature superconductivity by finding the cause for the T_c depression in the 123 compounds with Pr. The controversy, in addition to deciding the cause for the T_c decrease also concerns the Pr valance on the Pr ion site.

Illustrative of the complexity of the high-temperature superconductor materials is the phase diagram which applies to the cuprate materials. The gap shape is roughly similar to the BCS gap, but shows different peak shapes, and characteristic kinks. Normal-superconductor tunneling also show a reproducible background slope, favoring the tunneling of holes. Also, there does not seem to be a systematic correspondence between the gap and the critical temperature. This strongly contradicts conventional BCS theory: in BCS superconductors, the gap and critical temperature

1.4.2 Effects of Impurity and Magnetic Ordering on YBCO Superconductor

The exchange interaction between charge carriers (e.g.electrons) and magnetic impurities is accompanied by a spin-flip process: when an electron is in proximity of a magnetic impurity, the interaction triggers a flip of both their spins. If no dipole-dipole interaction is at work, the total spin of the subsystem electron + magnetic impurity is conserved. This spin-flip process has dramatic consequences for a superconductor. Indeed, in all known superconductors charge-carriers are paired coherently with fixed relative S^z component of the pair's total spin. In the case of singlet pairing the pair has e.g. spin up-down, whereas in a triplet state the spin configuration of the pair is up-up. The presence of magnetic impurities lead to the pair-breaking effect. In a singlet superconductor the pair breaks in to two electrons up or down which no longer belong to condensation. Removing pairs from the condensate through implantation of magnetic impurities in to a superconductor has thus several direct consequences for the superconducting state. For example, it leads to a reduction of the superconducting critical temperature, of the energy gap, of the critical magnetic field H_{c2} [27] or the Josephson critical current J_c [28]. To support our prediction for the existence of superconductivity and magnetic ordering in general and ferromagnetic order in particular, we shall address both experimental and theoretical approaches given by different researchers.

Mattias et al. [29] made the first experimental investigation on the close relation between Superconductivity and ferromagnetism. They suggested that various rare earth alloys show simultaneous superconductivity and dilute Ferromagnetism such as Lanthanum-Gadolinium alloys. The fact that Gd lowers the superconducting transition temperature, T_c of La was expected. For more dilute alloys it is difficult to identify the ferromagnetic transition, unless one must apply a field which destroys superconductivity. They concluded that superconductivity is not only destroyed by ferromagnetic ordering, but also by rather small amounts of magnetic impurities, and the exchange interaction between the spins, not the total angular momentum, of the impurity ions and conduction electron spins, was responsible for the depression of the superconducting transition temperature.

Singh and Sinha [30] studied the effect of magnetic ordering on superconductivity in some rare earth compound and found a reentrant behavior of the order parameter. They found that superconductivity can be destroyed at two temperatures T_{c1} due to thermal pair breaking and at T_{c2} when $\Delta = \varphi$, φ being related to magnetic ordering of rare earth ions and spin polarization of conduction electrons.

Kebede et al., [23] studied the magnetic and thermal transport and structural properties of alloy $Y_{1-x}Pr_xBa_2Cu_3O_{7-\delta}$. They found that superconducting transition temperature T_c is reduced while ordering temperature, T_m is increased by increasing Pr concentration below the critical value.

Theoretically, we can distinguish two regions of interest: One is the region above the concentration-dependent magnetic critical temperature T_m. For above T_m it is valid to assume that magnetic impurities are non-interacting. The second region of interest is $T < T_m$, where the interactions between magnetic impurities are strong and spontaneously magnetic ordering sets in. This case is more difficult to handle because there exist an additional exchange field acting on the conduction electron spins [31], and the conduction electrons are scattered by the excitation of the spin system [32]. These additional mechanisms lead to pair breaking in the superconducting state. For ferromagnetic ordering, it is difficult to modify AG theory in this region to account for the magnetic interactions because of these additional mechanisms [31, 32]. However, for antiferroagnetic or spin glass, where the average internal magnetic fields are small, the motion of the conduction electrons should not be affected. Gorkov and Rusinov [31] predicted the possibility of co-existence of superconductivity and ferromagnetism in a narrow temperature range.

Abrikosov and Gorkov [7] have discussed the effect of spin-flip scattering by impurities with localized moments on the superconducting properties. They have found that at a certain concentration of magnetic impurities the superconducting transition temperature T_c decreases linearly as a function of small concentration, and vanishes at a critical impurity concentration n_{AG}. However, near the magnetic transition, the assumption of noninteracting magnetic impurities break down. Modifications of the AG theory due to spatial spin correlations of both ferro and antiferromagnetic type have been considered. Once the impurities are added to the system, the effective energy gap may vanish for some critical concentration while the system still remains superconductivity leading to the so called gapless superconductivity. They [7] obtained an equation for T_c in the presence of magnetic impurity as

$$\ln\left(\frac{T_{co}}{T_c}\right) = \psi\left(\frac{1}{2} + \gamma_s\right) - \psi\left(\frac{1}{2}\right), \tag{1.4.2}$$

where, $\gamma_s = \frac{\Gamma_s T_c}{2\pi T_c}$x, and Γ_s is the spin-flip scattering amplitude, x is the magnetic impurity concentration and ψ is the digamma function.

Reif and Woolf [33], on the basis of tunneling experiments have experimentally demonstrated that there is a difference between the slopes in the transition temperature and in the effective energy gap as a function of the concentration of magnetic impurities, in accord with the prediction of the theory. Weiss et al. [34] have carried out more detailed calculations of the properties of superconductivity with magnetic impurities to determine the transition temperature T_c (Γ_s) and gap parameter Δ (Γ_s, T) as a function of parameter Γ_s, where $2\Gamma_s$ is the inverse relaxation time resulting from spin-flip scattering by magnetic impurities. The have also calculated the electrical conductivity at zero temperature.

1.4.3 Mechanisms of T_c suppression in $Y_{1-x}Pr_xBa_2Cu_3O_{7-\delta}$

The Pr analog of some rare-earth (R) high-T_c cuprate series has a unique suppressed superconductivity. The Pr analog has a behavior indistinguishable from the isostructral R-substituted members. So in $Y_{1-x}Pr_xBa_2Cu_3O_{7-\delta}$(YPBCO) system, T_c has been found to decrease monotonically from 92K with x=0 (x is Pr concentration) to 0K with x≈ 0.55 [35]. A number of experimental and theoretical investigations (mechanisms) have been done to explain the suppression of superconductivity by Pr, including hole filling by charge transfer from Pr to the CuO_2 planes, hole localizations, magnetic pair breaking, or hybridization [36]. To date, and despite of considerable effort, the real understanding of this system is still lacking. We provide an evidence that correlates a wide variety of these observations and provide insight in to the interaction between magnetism and superconductivity in Pr-containing copper oxide.

The first possible mechanism is hole filling (localization). In this experimental observation, if the valance of Pr is +4 or greater than +3, the additional electrons donated by Pr ion are expected to fill mobile holes in the CuO_2 planes, and thus destroy superconductivity. Magnetic [37], low temperature specific heat [38], and chemical-substitution investigations [39] are consistence with the existence of Pr^{4+}; Hall effect [37] and neutron diffraction [40] studies also support Pr valance greater than +3. However, electron-loss spectroscopy [41], X-ray absorption spectroscopy [42] and Nuclear magnetic resonance (NMR) [36] studies show a Pr valance close to +3 in the YPBCO system.

The second Possible mechanism is magnetic pair-breaking by local moments due to spin-dependent exchange scattering of the holes in the CuO_2 planes, with hybridization between the Pr $4f$ states and the CuO_2 valance-band states contributing as well. The main evidence for magnetic pair breaking is that the curve of T_c vs.

n in YPBCO appears to follow the Abrikosov-Gorkov(AG) pair breaking model [7]. That means the strong hybridization of Pr $4f$ with O $2p$ states leads to localization of the holes with out requiring a Pr formal valance greater than +3. But this alone is not sufficient to suppress superconductivity. However, a more accurate experiment gives that the T_c vs. n curve does not follow the AG theory strictly and there is no direct evidence for pair breaking in the experiments [43]. Obviously, the reason for the suppression of superconductivity in YPBCO is not clear.

Generally, studies of $Y_{1-x}Pr_xBa_2Cu_3O_{7-\delta}$ system afford one an opportunity to obtain important information about fundamental aspects of high-T_c oxides. Therefore, in this review we have seen that Pr ions play several important roles in doped host compound, which controls the concentration of mobile holes in the CuO_2 planes, allowing the relationship between T_c and mobile holes to be studied, and it carries a localized magnetic moment so that the interplay between superconductivity and magnetism can be explored. Additionally, Pr substitution allows T_c to be continually tuned between 92K and 0K, making it possible to test for scaling and universality of properties such as upper critical field, irreversibility line, and to the superconductivity energy gap by electron tunneling or infrared absorption for example, as T_c is varied. As the magnetic impurity order either directly and/or indirectly , the magnetic ordering temperature increases linearly and can show a possible coexistence of superconductivity and magnetism. This is investigated also in the present work and also the suppression of energy gap parameter.

Using Eqs. (2.1.4), (2.1.5) and (2.1.6) in Eq. (2.1.3), we have

$$\omega G^{r}_{\hat{A},\hat{B}}(\omega) =< [\hat{A}(t), \hat{B}(t')] >_{\omega} \ + \ \ll [\hat{A}(t), \hat{H}]; \hat{B}(t') \gg_{\omega} . \tag{2.1.7}$$

Here, $\ll ... \gg$ is the abbreviated notation for the the Fourier transform of the corresponding Green function, and $< ... >$ denotes averaging over a grand canonical ensemble. The commuting and anticommuting relation for the two operators is also given by

$$[\hat{A} \ \hat{B}] = \hat{A}\hat{B} - \eta \hat{B}\hat{A}, \tag{2.1.8}$$

where $\eta = 1$ for Boson operators, and $\eta = -1$ for Fermion Operators. That means, for two Boson operators:

$$[C_{k\sigma}, C^{+}_{k'\sigma'}] = C_{k\sigma}C^{+}_{k'\sigma'} \ - \ C^{+}_{k'\sigma'}C_{k\sigma} = \delta_{kk'}\delta_{\sigma\sigma'}, \tag{2.1.9}$$

and

$$[C_{k\sigma}, C_{k'\sigma'}] = [C^{+}_{k\sigma}, C^{+}_{k'\sigma'}] = 0. \tag{2.1.10}$$

For two Fermion operators:

$$\{C_{k\sigma}, C^{+}_{k'\sigma'}\} = C_{k\sigma}C^{+}_{k'\sigma'} \ + \ C^{+}_{k'\sigma'}C_{k\sigma} = \delta_{kk'}\delta_{\sigma\sigma'}, \tag{2.1.11}$$

and

$$\{C_{k\sigma}, C_{k'\sigma'}\} = \{C^{+}_{k\sigma}, C^{+}_{k'\sigma'}\} = 0. \tag{2.1.12}$$

The correlation function $< \hat{B}(t')\hat{A}(t) >$ is related to the analytic property of Green's function by

$$< \hat{B}(t')\hat{A}(t) >= i \lim_{\epsilon \to 0} \int_{-\infty}^{\infty} \frac{\left(\ll \hat{A}, \hat{B} \gg_{\omega + i\epsilon} - \ll \hat{A}, \hat{B} \gg_{\omega - i\epsilon} \right) \exp -\omega(t - t')d\omega}{\exp(\beta\omega) - 1}. \tag{2.1.13}$$

Now in order to obtain the superconductivity properties, we have defined superconducting order parameter, Δ (energy gap), which is pairing of opposite spins and momentum by

$$\Delta = \Sigma_k V < C_{k\uparrow} C_{-k\downarrow} >, \tag{2.1.14}$$

$$\Delta^* = \Sigma_k V < C^+_{-k\downarrow} C^+_{k\uparrow} >, \tag{2.1.15}$$

where $\Delta = \Delta^*$ (since Δ is real). The value of transition temperature T_c is calculated by using the condition, $T \to T_c$, as $\Delta \to 0$ from the BCS Hamiltonian, and is given by

$$\hat{H}_{BCS} = \sum_k C^+_{k\sigma} C_{k\sigma} - \Sigma_{kk'} V_{kk'} C^+_{k\uparrow} C^+_{-k\downarrow} C_{k'\downarrow} C_{-k'\uparrow}. \tag{2.1.16}$$

Using the reduced BCS Hamiltonian, the equation of motion for $\ll C_{k\uparrow}, C^+_{k\uparrow} \gg$ is given by

$$\omega \ll C_{k\uparrow}, C^+_{k\uparrow} \gg = \delta_{kk'} + \ll [c_{k\uparrow}, \hat{H}_{BCS}]; C^+_{k\uparrow} \gg . \tag{2.1.17}$$

From Eq. (2.1.17), the higher order Green function can also be found

$$\ll C^+_{-k\downarrow} C^+_{k\uparrow} \gg = \left(\frac{-\Delta}{\omega^2 - \varepsilon_k^2 - \Delta^2} \right). \tag{2.1.18}$$

The superconducting order parameter Δ, is also given by the relation

$$\Delta = \frac{V}{\beta} \Sigma_{nk} \ll C^+_{-k\downarrow} C^+_{k\uparrow} \gg . \tag{2.1.19}$$

Equating Eq. (2.1.18) and (2.1.19), and converting summation over k into an integral with cutoff energy $\pm\hbar\omega_b$ from the Fermi level, it becomes

$$\Delta = N(0)V \int_{-\hbar\omega_b}^{\hbar\omega_b} \left(\frac{\Delta \tanh \frac{\beta}{2} (\varepsilon_k^2 + \Delta^2)^{1/2}}{2(\varepsilon_k^2 + \Delta^2)^{1/2}} \right) d\varepsilon_k. \tag{2.1.20}$$

If we put $\Delta \to 0$, as $T \to T_c$, then Eq.(2.1.20) has the form

$$\frac{1}{N(0)V} = \int_0^{\hbar\omega_b} \left(\frac{\tanh \frac{1}{2}\beta\varepsilon_k}{\varepsilon_k} \right) d\varepsilon_k. \tag{2.1.21}$$

After evaluating the above integral, we get

$$T_c = 1.14\omega_b \exp\left(\frac{-1}{N(0)V}\right), \tag{2.1.22}$$

where, $\beta = \frac{1}{k_BT}$, $N(0)$ is the density of state at the Fermi level, and ω_b is the the excitation frequency, like Bosons. We assumed to put $\hbar = k_B$=1 for our mathematical formulation.

2.2 Mean Field Theory of Ferromagnetism

One possibility to describe observed properties of magnetic structure is to start with Heisenberg spin Hamiltonian. Although no complete solution has been found even to this simplified problem, it is possible to extract much partial information in a variety of important cases, with two interesting approaches like the spin wave theory, and the molecular field theory. Now we are primarily concerned, the mean field or molecular field theory, which is of our interest to obtain magnetic ordering temperature in the second part of the formalism. First, it is indispensable to remember the concept of magnetic susceptibility. When we vary the external applied magnetic field H acting on a solid, its change of magnetization M will be a function of the temperature T is

$$\chi(T) = \lim_{|H|\to 0}\left(\frac{\partial \mathrm{M}}{\partial \mathrm{H}}\right). \tag{2.2.1}$$

The susceptibility χ of a solid is measured and it is used to categorize different kinds of solids like ferromagnets, in which all magnetic moments are in parallel alignment, antiferromagnets, in which adjacent magnetic moments lie in antiparallel alignment, spiral and helical structures in which the direction of magnetic moment processes around a cone or a circle as one moves from one site to the next, and spin glasses in which the magnetic moments lie in frozen random arrangements. The starting point in many treatments of ferromagnetism is to treat the interaction of an atomic moment with its neighboring atomic moments as if it were an additional component of the magnetic field, and no account taken of vibrations (fluctuations) from site to site. The effective field measures the effect of ordering of the system experienced by each atomic site is, and therefore given by

$$\mathbf{H}_{eff} = \mathbf{H} + \lambda \mathbf{M}, \tag{2.2.2}$$

where $\lambda > 0$, is a constant which parameterize the strength of the molecular field as a function of the magnetization. The mean magnetic moment, or magnetization for N atoms is also given by

$$M = N \sum_i \mu_i p_i = N \frac{\sum_{-s}^{s} (-m_s g \mu_B) e^{-\beta m_s g H_{eff}}}{\sum_{-s}^{s} e^{-\beta \mu_B g H_{eff}}}$$

$$= N g \mu_B S B_s(x), \tag{2.2.3}$$

where $B_s(x)$ is the Brillouin function, which is given by

$$B_s(x) = \frac{1}{S}\left[(S+\frac{1}{2})\coth[(S+\frac{1}{2})x] - \frac{1}{2}\coth\frac{x}{2}\right], \tag{2.2.4}$$

and $x = \frac{g\mu_B H_{eff}}{k_B T}$, and g is the Land'e factor which depends on the magnitude of L and S, given by

$$g = \left(1 + \frac{J(J+1) + S(S+1) - L(L+1)}{2J(J+1)}\right). \tag{2.2.5}$$

For $x \ll 1$, $B_s(x)=\frac{(S+1)x}{3}$, and using $H_{eff} = H + \lambda M$, we have a self-consistent equation for M as

$$M = \left(\frac{N g^2 \mu_B^2 S(S+1)(H + \lambda M)}{3 k_B T}\right). \tag{2.2.6}$$

Re-writing Eq. (2.2.6) as

$$M\left[1 - \frac{C\lambda}{T}\right] = \left(\frac{C}{T}\right)H. \tag{2.2.7}$$

Chapter 3

MODELS AND THEORETICAL FORMALISM

The interplay of superconductivity and magnetism has attracted the attention of many solid state physicists. The effect of a single magnetic impurity on the superconductivity has been well understood. However, the effect of highly concentrated magnetic ions on the superconductivity is still open to question in spite of a considerable efforts. This is partly because there is existed no stoichiometric compound suitable for studying this problem. The objective of this thesis is to study theoretically the coexistence of magnetic and superconducting properties of Pr doped cuprate by constructing model Hamiltonian in this chapter. Let us consider a system of conduction electrons and an impurity on which a magnetic moment is localized in a very small region. The so called sd exchange interaction acts between the conduction electrons and the localized moment. Thus, with the frame work of BCS model, the Hamiltonian of a superconductor containing magnetic impurity is given by

$$\hat{H} = H_0 + \hat{H}_{BCS} + \hat{H}_{s-f} + \hat{H}_{ff}. \tag{3.0.1}$$

where $\hat{H}_{s-f}$ is the the exchange interaction between conduction electrons and impurity spins, which is given by

$$\hat{H}_{s-f} = \frac{-J}{N}\sum_{jkk'} e^{i(\mathrm{K}-\mathrm{K}').\mathrm{R}_j}\Big((C_{k\uparrow}^{+}C_{k'\uparrow} - C_{k\downarrow}^{+}C_{k'\downarrow})S_j^z + C_{k\uparrow}^{+}C_{k'\downarrow}S_j^{+} + C_{k\downarrow}^{+}C_{k'\uparrow}S_j^{-}\Big), \tag{3.0.2}$$

and $\hat{H}_{ff}$ is the direct Heisenberg exchange of localized spins, which is given by

$$\hat{H}_{ff} = \sum_{ij} J_{ij}\mathrm{S}_i.\mathrm{S}_j = \sum_{ij} J_{ij}\Big(S_i^z S_j^z + \frac{1}{2}S_i^{+}S_j^{-} + \frac{1}{2}S_i^{-}S_j^{+}\Big). \tag{3.0.3}$$

And H_0 is the kinetic energy of the conduction electrons, and $\hat{H}_{BCS}$ is the model Hamiltonian of BCS which describes the superconducting state of the conduction electrons, and they can be expressed as,

$$H_0 + \hat{H}_{BCS} = \sum_k \varepsilon_k\Big(C_{k\uparrow}^{+}C_{k\uparrow} + C_{k\downarrow}^{+}C_{k\downarrow}\Big) - \sum_{kk'} V_{kk'}C_{k\uparrow}^{+}C_{-k\downarrow}^{+}C_{k'\downarrow}C_{-k'\uparrow}, \tag{3.0.4}$$

where $C_{k\sigma}^{+}$ and $C_{k\sigma}$, are creation and destruction operators for conduction electrons of momentum k, energy ε_k and spin σ. ε_k is measured from the Fermi level of the pure metal. S^z and $S^{\pm}$ are the components of the spin operators of the impurity, and N is the total number of atoms in the crystal, J is the coupling constant of the s-f exchange interaction, J_{ij} is the exchange integral between the i^{th} and j^{th} localized ion, and equal to J for nearest-neighboring, $e^{i(\mathrm{k}-\mathrm{k}').\mathrm{R}_j}$ is a plane-wave state (normalized to the total volume). $C_{k\uparrow}^{+}C_{K'\uparrow}$ and $C_{k\downarrow}^{+}C_{k'\downarrow}$ are the spins of conduction electron up and down in the scattering interaction respectively, $C_{k\uparrow}^{+}C_{k'}\downarrow S_j^{+}$ and $C_{k\downarrow}^{+}C_{k'\uparrow}S_j^{-}$ are represent spin- flip process, where there is a mutual spin-flip between the conduction and the local spin.

3.1 Energy gap versus T_c Formulation

In this section our goal is to find correlations among electrons/holes; energy gap, and impurity transition temperature T_c'. Using the Green's function approach the equation of motion for $\ll C_{k\uparrow}, c^+_{k'\uparrow} \gg$ is given by

$$\omega \ll C_{k\uparrow}, C^+_{k'\uparrow} \gg = \delta_{kk'} + \ll [C_{k\uparrow}, \hat{H}]; c^+_{k'\uparrow} \gg . \tag{3.1.1}$$

And, now let us evaluate the following Commuting relations:

$$\begin{aligned}
[C_{k\uparrow}, H_0] &= \sum_p \varepsilon_p \Big([C_{k\uparrow}, C^+_{p\uparrow} C_{p\uparrow}] + [C_{k\uparrow}, C^+_{p\downarrow} C_{p\downarrow}] \Big) \\
&= \sum_p \varepsilon_p \Big([C_{k\uparrow}, C^+_{p\uparrow} C_{p\uparrow}] \Big) \\
&= \sum_p \varepsilon_p \Big(\{C_{k\uparrow}, C^+_{p\uparrow}\} C_{p\uparrow} - C^+_{p\uparrow} \{C_{k\uparrow}, C_{p\uparrow}\} \Big) \\
&= \sum_p \varepsilon_p \{C_{k\uparrow}, C^+_{p\uparrow}\} C_{p\uparrow} \\
&= \sum_p \varepsilon_p \delta_{kp} C_{p\uparrow} \\
&= \varepsilon_k C_{k\uparrow}.
\end{aligned} \tag{3.1.2}$$

$$\begin{aligned}
[C_{k\uparrow}, \hat{H}_{BCS}] &= -\sum_{pk'} V_{pk'} \Big[C_{k\uparrow}, C^+_{p\uparrow} C^+_{-p\downarrow} C_{k'\downarrow} C_{-k'\uparrow} \Big] \\
&= \sum_{pk'} V_{pk'} \Big(C^+_{p\uparrow} C^+_{-p\downarrow} \Big[C_{k\uparrow}, C_{k'\downarrow} C_{-k'\uparrow} \Big] + \Big[C_{k\uparrow}, C^+_{p\uparrow} C^+_{-p\downarrow} \Big] C_{k'\downarrow} C_{-k'\uparrow} \Big) \\
&= \sum_{pk'} V_{pk'} \Big[C_{k\uparrow}, C^+_{p\uparrow} C^+_{-p\downarrow} \Big] C_{k'\downarrow} C_{-k'\uparrow} \\
&= \sum_{pk'} V_{pk'} \Big(\{C_{k\uparrow}, C^+_{p\uparrow}\} C^+_{-p\downarrow} - C^+_{p\uparrow} \{C_{k\uparrow}, C^+_{-p\downarrow}\} \Big) C_{k'\downarrow} C_{-k'\uparrow} \\
&= -\sum_{pk'} V_{pk'} C^+_{-p\downarrow} \delta_{kp} C_{k'\downarrow} C_{-k'\uparrow} \\
&= -\sum_{k'} V_{k'} C^+_{-k\downarrow} C_{k'\downarrow} C_{-k'\uparrow}.
\end{aligned} \tag{3.1.3}$$

$$[C_{k\uparrow},\hat{H}_{s-f}] = \frac{-J}{N}\sum_{jkk'} e^{i(\mathbf{k}-\mathbf{k}').\mathbf{r}_j}\Big(S^z_j([C_{k\uparrow},C^+_{k\uparrow}C_{k'\uparrow}]-[C_{k\uparrow},C^+_{k\downarrow}C_{k'\downarrow}])+S^+_j[C_{k\uparrow},C^+_{k\uparrow}C_{k'\downarrow}]$$

$$+S^-_j[C_{k\uparrow},C^+_{k\downarrow}C_{k'\uparrow}]\Big)$$

$$= \frac{-J}{N}\sum_{jkk'} e^{i(\mathbf{k}-\mathbf{k}').\mathbf{r}_j}\Big(S^z_j(\{C_{k\uparrow},C^+_{k\uparrow}\}C_{k'\uparrow}-C^+_{k\uparrow}\{C_{k\uparrow},C_{k'\uparrow}\})$$

$$+S^+_j(\{C_{k\uparrow},C^+_{k\uparrow}\}C_{k'\downarrow}-C^+_{k\uparrow}\{C_{k\uparrow},C_{k'\downarrow}\})$$

$$+S^-_j(\{C_{k\uparrow},C^+_{k\downarrow}\}C_{k'\uparrow}-C^+_{k\downarrow}\{C_{k\uparrow},C_{k'\uparrow}\})\Big)$$

$$= \frac{-J}{N}\sum_{jkk'} e^{i(\mathbf{k}-\mathbf{k}').\mathbf{r}_j}(S^z_j\delta_{kk}C_{k'\uparrow}+S^+_j\delta_{kk}C_{k'\downarrow})$$

$$= \frac{-J}{N}\sum_{jkk'} e^{i(\mathbf{k}-\mathbf{k}').\mathbf{r}_j}(S^z_jC_{k'\uparrow}+S^+_jC_{k'\downarrow}). \quad (3.1.4)$$

$$[C_{k\uparrow},\hat{H}_{ff}] = \sum_{ij} J_{ij}\Big([C_{k\uparrow},S^z_iS^z_j+\frac{S^+_iS^-_j}{2}+\frac{S^-_iS^+_j}{2}]\Big) = 0. \quad (3.1.5)$$

Substituting from Eq. (3.1.2) to (3.1.5) in Eq. (3.1.1), we get

$$(\omega-\varepsilon_k) \ll C_{k\uparrow},C^+_{k'\uparrow}\gg = \delta_{kk'} - \sum_{k'} V_{k'} \ll C^+_{-k\downarrow}C_{k'\downarrow}C_{-k'\uparrow},C^+_{k'\uparrow}\gg$$

$$\frac{-J}{N}\sum_{jkk'} e^{i(\mathbf{k}-\mathbf{k}').\mathbf{r}_j}\Big(\ll S^z_jC_{k'\uparrow},C^+_{k'\uparrow}\gg+\ll S^+_jC_{k'\downarrow},C^+_{k'\uparrow}\gg\Big). \quad (3.1.6)$$

Using Wick's theorem, we have

$$\ll C^+_{-k\downarrow}C_{k'\downarrow}C_{-k'\uparrow},C^+_{k'\uparrow}\gg \cong < C_{k'\downarrow}C_{-k'\uparrow}> \ll C^+_{-k\downarrow},C^+_{k'\uparrow}\gg, \quad (3.1.7)$$

and from Tyablikov decoupling

$$\ll S^z_jC_{k'\uparrow},C^+_{k'\uparrow}\gg \cong < S^z_j > \ll C_{k'\uparrow}C^+_{k'\uparrow}\gg, \quad (3.1.8)$$

$$\ll S_j^+ C_{k'\downarrow}, C_{k'\uparrow}^+ \gg \cong < S_j^+ > \ll C_{k'\downarrow}, C_{k'\uparrow}^+ \gg . \tag{3.1.9}$$

But we have already defined the energy gap as

$$\Delta = \Sigma_{k'} V_{k'} < C_{k'\downarrow} C_{-k'\uparrow} > . \tag{3.1.10}$$

And we assumed that our direction of quantization is along z-axis so that

$$< S_j^+ > \cong 0. \tag{3.1.11}$$

$$< S_j^z > \cong nS, \tag{3.1.12}$$

where n is the number of impurity added. Thus, using from Eq. (3.1.7) to (3.1.12) in Eq. (3.1.6), we have

$$(\omega - \varepsilon_k) \ll C_{k\uparrow}, C_{k'\uparrow}^+ \gg = \delta_{kk'} - \Delta \ll C_{-k\downarrow}^+, C_{k'\uparrow}^+ \gg$$

$$-\frac{nJS}{N} \sum_{jkk'} e^{i(\mathbf{k}-\mathbf{k}').\mathbf{r}_j} \ll C_{k'\uparrow}, C_{k'\uparrow}^+ \gg . \tag{3.1.13}$$

Again the equation of motion for the Green's function $\ll C_{-k\downarrow}^+, C_{k'\uparrow}^+ \gg$ is also given by

$$\omega \ll C_{-k\downarrow}^+, C_{k'\uparrow}^+ \gg = < [C_{-k\downarrow}^+, C_{k'\uparrow}^+] > + \ll [C_{-k\downarrow}^+, \hat{H}], C_{k'\uparrow}^+ \gg . \tag{3.1.14}$$

Similarly,

$$\begin{aligned}
[C_{-k\downarrow}^+, H_0] &= \sum_p \varepsilon_p \Big([C_{-k\downarrow}^+, C_{p\uparrow}^+ C_{p\uparrow} + C_{p\downarrow}^+ C_{p\downarrow}] \Big) \\
&= \sum_p \varepsilon_p \Big(\{C_{-k\downarrow}^+, C_{p\downarrow}^+\} C_{p\downarrow} - C_{p\downarrow}^+ \{C_{-k\downarrow}^+, C_{p\downarrow}\} \Big) \\
&= -\sum_p \varepsilon_p C_{p\downarrow}^+ \delta_{-kp} \\
&= -\varepsilon_{-k} C_{-k\downarrow}^+ .
\end{aligned} \tag{3.1.15}$$

$$[C^+_{-k\downarrow}, \hat{H}_{BCS}] = -\sum_{pk'} V_{pk'} [C^+_{-k\downarrow}, C^+_{p\uparrow} C^+_{-p\downarrow} C_{k'\downarrow} C_{-k'\uparrow}]$$

$$= -\sum_{pk'} V_{pk'} \Big(C^+_{p\uparrow} C^+_{-p\downarrow} [C^+_{-k\downarrow}, C_{k'\downarrow} C_{-k'\uparrow}] + [C^+_{-k\downarrow}, C^+_{p\uparrow} C^+_{-p\downarrow}] C_{k'\downarrow} C_{-k'\uparrow} \Big)$$

$$= -\sum_{pk'} V_{pk'} C^+_{p\uparrow} C^+_{-p\downarrow} \Big(\{C^+_{-k\downarrow}, C_{k'\downarrow}\} C_{-k'\uparrow} - C_{k'\downarrow} \{C^+_{-k\downarrow}, C_{-k'\uparrow}\} \Big)$$

$$= -\sum_{pk'} V_{pk'} C^+_{p\uparrow} C^+_{-p\downarrow} C_{-k'\uparrow} \delta_{-kk'}$$

$$= -\sum_{p} V_p C^+_{p\uparrow} C^+_{-p\downarrow} C_{k\uparrow}. \tag{3.1.16}$$

$$[C^+_{-k\downarrow}, \hat{H}_{s-f}] = \frac{-J}{N} \sum_{jkk'} e^{i(\mathbf{k}-\mathbf{k}').\mathbf{r}_j} \Big(S^z_j ([C^+_{-k\downarrow}, C^+_{k\uparrow} C_{k'\uparrow}] - [C^+_{-k\downarrow}, C^+_{k\downarrow} C_{k'\downarrow}])$$

$$+ S^+_j [^+_{-k\downarrow}, C^+_{k\uparrow} C_{k'\downarrow} + S^-_j [C^+_{-k\downarrow}, C^+_{k\downarrow} C_{k'\uparrow}] \Big)$$

$$= \frac{-J}{N} \sum_{jkk'} e^{i(\mathbf{k}-\mathbf{k}').\mathbf{r}_j} \Big(-S^z_j (\{C^+_{-k\downarrow}, C^+_{k\downarrow}\} C_{k'\downarrow} - C^+_{k\downarrow} \{C^+_{-k\downarrow}, C_{k'\downarrow}\})$$

$$+ S^+_j (\{C^+_{-k\downarrow}, C^+_{k\uparrow}\} C_{k'\downarrow} - C^+_{k\uparrow} \{C^+_{-k\downarrow}, C_{k'\downarrow}\})$$

$$+ S^-_j (\{C^+_{-k\downarrow}, C^+_{k\downarrow}\} C_{k'\uparrow} - C^+_{k\downarrow} \{C^+_{-k\downarrow}, C_{k'\uparrow}\}) \Big)$$

$$= \frac{-J}{N} \sum_{jkk'} e^{i(\mathbf{k}-\mathbf{k}').\mathbf{r}_j} \Big(S^z_j C^+_{k\downarrow} \delta_{-kk'} - S^+_j C^+_{k\uparrow} \delta_{-kk'} \Big). \tag{3.1.17}$$

$$[C^+_{-k\downarrow}, \hat{H}_{ff}] = \sum_{ij} J_{ij} \Big(\Big[C^+_{-k\downarrow}, S^z_i S^z_j + \frac{S^+_i S^-_j}{2} + \frac{S^-_i S^+_j}{2} \Big] \Big) = 0. \tag{3.1.18}$$

Substituting from Eq. (3.1.15) to (3.1.18) in Eq. (3.1.14), we get

$$(\omega + \varepsilon_{-k}) \ll C^{+}_{-k\downarrow}, C^{+}_{k'\uparrow} \gg = -\sum_{p} V_p \ll C^{+}_{p\uparrow} C^{+}_{-p\downarrow} C_{k\uparrow}, C^{+}_{k'\uparrow} \gg$$

$$-\frac{J}{N} \sum_{jkk'} e^{i(\mathbf{k}-\mathbf{k}').\mathbf{r}_j} \Big(\ll S^{z}_{j} C^{+}_{k\downarrow} \delta_{-kk'}, C^{+}_{k'\uparrow} \gg \Big)$$

$$+\frac{J}{N} \sum_{jkk'} e^{i(\mathbf{k}-\mathbf{k}').\mathbf{r}_j} \Big(\ll S^{+}_{j} C^{+}_{k\uparrow} \delta_{-kk'}, C^{+}_{k'\uparrow} \gg \Big). \quad (3.1.19)$$

Again using the Wick's theorem and Tyablikov decoupling, we can approximate the above terms as

$$\ll C^{+}_{p\uparrow} C^{+}_{-p\downarrow} C_{k\uparrow}, C^{+}_{k'\uparrow} \gg \cong < C^{+}_{p\uparrow} C^{+}_{-p\downarrow} > \ll C_{k\uparrow}, C^{+}_{k'\uparrow} \gg, \quad (3.1.20)$$

$$\ll S^{z}_{j} C^{+}_{k\downarrow} \delta_{-kk'}, C^{+}_{k'\uparrow} \gg \cong \delta_{-kk'} < S^{z}_{j} > \ll C^{+}_{k\downarrow}, C^{+}_{k'\uparrow} \gg, \quad (3.1.21)$$

and

$$\ll S^{+}_{j} C^{+}_{k\uparrow} \delta_{-kk'}, C^{+}_{k'\uparrow} \gg \cong \delta_{-kk'} < S^{+}_{j} > \ll C^{+}_{k\uparrow}, C^{+}_{k'\uparrow} \gg . \quad (3.1.22)$$

And, we also define the energy gap as

$$\Delta^{*} = -\sum_{p} V_p < C^{+}_{p\uparrow} C^{+}_{-p\downarrow} >, \quad (3.1.23)$$

but $\Delta = \Delta^{*}$ (since gap parameter is real), and $\frac{1}{N} \sum_{jkk'} e^{i(\mathbf{k}-\mathbf{k}').\mathbf{r}_j} = \delta(k - k')$ is an oscillating plane wave, and has a maximum average value at $\mathbf{k} = \mathbf{k}'$. Thus, using $\mathbf{k} = \mathbf{k}'$ in Eq. (3.1.13), and substituting from Eq. (3.1.20) to (3.1.23) in Eq. (3.1.19), we have

$$(\omega - \varepsilon_k + nSJ) \ll C_{k\uparrow}, C^{+}_{k\uparrow} \gg = 1 - \Delta \ll C^{+}_{-k\downarrow}, C^{+}_{k\uparrow} \gg, \quad (3.1.24)$$

$$(\omega + \varepsilon_{-k} + nSJ) \ll C^{+}_{-k\downarrow}, C^{+}_{k\uparrow} \gg = -\Delta^{*} \ll C_{k\uparrow}, C^{+}_{k\uparrow} \gg . \quad (3.1.25)$$

Equating the above two equations, we get

$$\Big((\omega - \varepsilon_k + nSJ)(\omega + \varepsilon_{-k} + nSJ) - \Delta^2\Big) \ll C^+_{-k\downarrow}, C^+_{k\uparrow} \gg = -\Delta, \qquad (3.1.26)$$

but $\varepsilon_k = \varepsilon_{-k}$ is the kinetic energy of conduction electrons, and Eq. (3.1.26) becomes

$$\ll C^+_{-k\downarrow}, C^+_{k\uparrow} \gg = \frac{-\Delta}{\omega^2 - \varepsilon_k^2 + 2\omega nSJ + (nSJ)^2 - \Delta^2}. \qquad (3.1.27)$$

Let us define $\omega'^2 = (\omega + nSJ)^2$, which is the new vibrational frequency because of the added magnetic impurity. The gap parameter is already defined by

$$\Delta = \frac{V}{\beta} \sum_{nk} \ll C^+_{-k\downarrow}, C^+_{k\uparrow} \gg . \qquad (3.1.28)$$

Now changing, $\omega' \rightarrow i\omega'_{n'}$, and using the Matsubara frequency expression for fermions by

$\omega'_{n'} = \frac{(2n'+1)\pi}{\beta}$, Eq. (3.1.27) is reduced to

$$\Delta = \frac{V}{\beta} \sum_{n'k} \frac{\Delta}{\Delta^2 - 2(nSJ)^2 + \varepsilon_k^2 + \frac{(2n'+1)^2\pi^2}{\beta^2}}. \qquad (3.1.29)$$

If we consider, $(\Delta^2 - 2(nSJ)^2 + \varepsilon_k^2) = x^2$, then Eq. (3.1.29) becomes

$$1 = \sum_{n'k} V\beta \frac{1}{\beta^2 x^2 + (2n'+1)^2\pi^2}. \qquad (3.1.30)$$

For calculational convenience, let us apply the formula of

$$\frac{\tanh y/2}{2y} = \sum_{n'=-\infty}^{\infty} \frac{1}{(2n'+1)^2\pi^2 + y^2}. \qquad (3.1.31)$$

Substituting Eq. (3.1.31) in Eq. (3.1.30), we get

$$1 = V \sum_k \frac{\tanh \beta/2\sqrt{\varepsilon_k^2 + \Delta^2 - 2(nSJ)^2}}{\sqrt{\varepsilon_k^2 + \Delta^2 - 2(nSJ)^2}}. \qquad (3.1.32)$$

The additional term in Eq. (3.1.32) is due to the magnetic impurity added, and we possibly modify the new gap parameter as

$$\Delta'^2 = \Delta^2 - 2(nSJ)^2. \qquad (3.1.33)$$

When changing the summation and integrating Eq. (3.1.32) from $-\hbar\omega_b$ to $\hbar\omega_b$,

$$1 = \lambda \int_0^{\hbar\omega_b} d\varepsilon_k \frac{\tanh \beta/2\sqrt{\varepsilon_k^2 + \Delta'^2}}{\sqrt{\varepsilon_k^2 + \Delta'^2}}, \tag{3.1.34}$$

where $\lambda = N_0 V$ is the normalized e-b coupling constant, and $\beta = \frac{1}{k_B T}$, and k_B is Boltzmann constant, ω_b is the vibrational frequency because of bosonic excitation, and N_0 is the energy density of state referring one spin only.

3.2 Magnetic Ordering Temperature (T_m)

In this part of our formalism we are trying to find the expression for magnetic ordering temperature versus impurity concentration, which is optimally doped to the host system not to destroy superconducting properties totally. In order to produce magnetic ordering effect, the spins must interact each other, even though they are localized , and having zero angular momentum. The exchange interaction of spins is an indirect RKKY [44] interaction mediated by the conduction electrons. Thus, the exchange coupling between a conduction spins σ and the 4f spins takes the form

$$\hat{H}_{s-f} = -\sum_j J(\mathrm{r} - \mathrm{r}_j)\ \sigma.\mathrm{S}_j. \tag{3.2.1}$$

It is the two-ion couplings which are primarily responsible for co-operative effects and magnetic ordering in the rare earths, and of this most important is the indirect exchange, by which the moments on pairs of ions are coupled through the intermediary of the conduction electrons. Now, we are able to treat the problem as if the system were in a simple paramagnetic field $\mathrm{H}_{eff} = \mathrm{H} + \mathrm{H}_j$, where H and H_j are the external field (which is zero in our treatment) and molecular field respectively. At low temperature, the moments can be aligned by the internal molecular field and producing self-sustaining magnetic order. But as the temperature is raised, thermal fluctuations begin to progressively destroy the magnetization and at the critical temperature, the order will be destroyed (Weiss model of Ferromagnetism). From Eq. (3.2.1), we have the spin-spin interaction of the localized 4f electrons, and using Heisenberg Hamiltonian for this interaction is given by

$$\hat{H}_{ff} = \sum_{ij} J_{ij}\mathbf{S}_i.\mathbf{S}_j. \tag{3.2.2}$$

Since the effective molecular field $\mathbf{H}_j$ is produced by the neighboring spins in the absence of external field, the exchange interaction can be replaced by the effective Hamiltonian, which is given by

$$\hat{H}_{eff} = -g\mu_B \sum_j \mathbf{H}_j\ .\mathbf{S}_j = -\int \mathbf{H}_j(\mathbf{r})\ .\mu(\mathbf{r})d\mathbf{r}. \tag{3.2.3}$$

Using Eqs. (3.2.2) and (3.2.3), the local magnetic field on site $\mathbf{r_j}$ is given by

$$\mathbf{H}_{eff}(j) = -\frac{1}{g\mu_B}\sum_i J_{ij} < \mathbf{S}_i > . \tag{3.2.4}$$

Similarly,

$$\mathbf{H}_{eff}(i) = -\frac{1}{g\mu_B}\sum_j J_{ij} < \mathbf{S}_j > . \tag{3.2.5}$$

The local field on site $\mathbf{r}_i$ induced moment at site $\mathbf{r}_j$, which is given by

$$\mu_j = \sum_i \chi_{ji}\mathbf{H}_i, \tag{3.2.6}$$

where χ_{ji} is the non-local magnetic susceptibility for the conduction electrons. Thus, for free-electron model, χ_{ji} is scalar (case of isotropy and translational invariance), such that

$$\chi_{ji} = \chi_{ij} = \chi(\mathbf{r_{ij}}) = \chi(r_{ij}). \tag{3.2.7}$$

The energy associated with the non-local field $\mathbf{H_j}$ (i.e effective exchange interaction) is

$$\varepsilon = -\frac{1}{2}\sum_j \mu_\mathrm{j}.\mathbf{H}_j$$

$$= -\frac{1}{2}\sum_{ij}\chi(r_{ij})\mathrm{H}_i.\mathrm{H}_j$$

$$= -\frac{1}{g^2\mu_B^2}J_{ij}^2\chi(r_{ij}) < S_i >< S_j > . \tag{3.2.8}$$

The effective magnetic field acting on the impurity $\mathbf{S}_i$ is given by

$$-g\mu_B H_{eff} < S_i >= -\frac{1}{g^2\mu_B^2}J^2(r_i - r_j)\chi(r_i - r_j) < S_i >< S_j > . \tag{3.2.9}$$

Assume that the Fourier transform of $J(r_i - r_j)$ can be expressed as

$$J(r_i - r_j) = J(0)\delta(r_i - r_j), \tag{3.2.10}$$

where $J(0)$ is the amplitude in RKKY interaction. Using Eqs. (3.2.9) and (3.2.10), we have

$$g\mu_B H_{eff} = \frac{1}{g^2\mu_B^2}J^2(0)\chi(\mathrm{q}) < S_j >, \tag{3.2.11}$$

where $\chi(\mathrm{q})$ is the magnetic susceptibility in momentum space.

Assuming that the spontaneous magnetization, which is a measure of magnetic ordering to be in the z-direction, we have

$$< S_j >\cong M = n < \mu_z >, \tag{3.2.12}$$

where μ_z is the component of the magnetic moment in the direction of molecular field which alone makes a contribution of the energy of the sum-over-states for a grand canonical ensemble, and is given by

$$Z = \sum_i e^{-\beta\varepsilon_i}, \tag{3.2.13}$$

where $\varepsilon_i = -\mu.\mathrm{H}_{eff} = -g\mu_B H_{eff} m_s$, and m_s varies from -S, -S+1, -S+2, ... S, and let $x = g\beta\mu_B H_{eff}$, the above equation can have the form

$$Z = \sum_{-s}^{s} e^{xm_s}. \tag{3.2.14}$$

Now let us expand the summation as

$$Z = e^{-sx} + e^{-sx}e^{x} + e^{-sx}e^{2x} + ...e^{sx}, \tag{3.2.15}$$

and

$$Z\ e^{x} = e^{-sx}e^{x} + e^{-sx}e^{2x} + e^{-sx}e^{3x} + ...e^{sx}e^{x}. \tag{3.2.16}$$

Subtracting Eq. (3.2.15) from Eq. (3.2.16), we have

$$Z = \frac{e^{-sx} - e^{sx}e^{x}}{1 - e^{x}} = \frac{e^{(s+1/2)x} - e^{-(s+1/2)x}}{e^{x/2} - e^{-x/2}} = \frac{\sinh(s+1/2)x}{\sinh(x/2)}. \tag{3.2.17}$$

The mean magnetic moment is also calculated by

$$< \mu_z >= \frac{1}{\beta}\frac{\partial \ln z}{\partial H_{eff}} = \frac{1}{\beta}\frac{\partial \ln z}{\partial x}\frac{\partial x}{\partial H_{eff}} = g\mu_B s B_s(x), \tag{3.2.18}$$

where $B_x(x)$ is the Brillouin function, which is given by

$$B_x(x) = \frac{1}{s}\left((s+1/2)\coth(s+1/2)x - \frac{1}{2}\coth(x/2)\right). \tag{3.2.19}$$

In the vicinity of magnetic transition temperature T_m the spontaneous magnetization is small, that means in paramagnetism we are dealing with low field strengths, so that the magnetic $g\mu_B H_{eff}$ is very much smaller than the thermal energy $k_B T$, so that $\frac{g\mu_B H_{eff}}{k_B T} \ll 1$, and we can expand $\coth(x)$ as

$$\coth(x) = \frac{1}{x} + \frac{x}{3} + ... \tag{3.2.20}$$

Using the above $\coth(x)$ expansion and leaving the higher order terms to the Brillouin function, the spontaneous magnetization, $< S_j >$ is evaluated as

$$< S_j >= n < \mu_z >= \frac{g^2 n(\mu_B)^2 H_{eff} S(S+1)}{3k_B T}. \qquad (3.2.21)$$

Substituting Eq. (3.2.21) in Eq. (3.2.11), we have

$$< S_q >= \frac{S(S+1)J^2(0)n\chi(q) < S_q >}{3g\mu_B k_B T}. \qquad (3.2.22)$$

Now T_m is defined as the higher temperature for which a non-zero Fourier components $< S_q >$ exists, thus we have

$$T_m = \frac{S(S+1)J^2(0)n\chi(\mathrm{Q})}{3gk_B\mu_B}. \qquad (3.2.23)$$

Here, Q is a wave vector for which χ maximum as shown in Fig. (3.1). This figure presents a schematic representation of the Q dependence of conduction-electron susceptibility for the normal and superconducting state, calculated by Ramakrishnan and Varma [45]. Where n is the concentration of magnetic impurity. It is worth noticing that while $nS(S+1)$ depends on the Pr ions, $J^2(0)$ depends both the Pr ions and Y-based system.

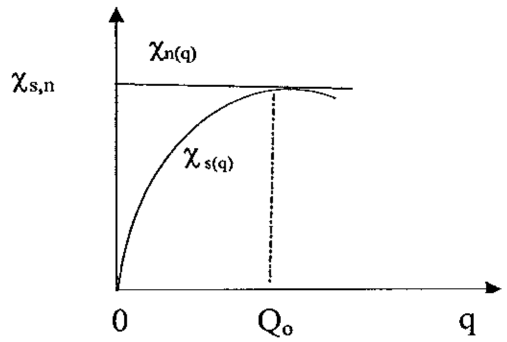

Figure 3.1: Electronic susceptibility χ_s and χ_n in the superconducting and normal state at T=0 respectively.

Chapter 4

RESULTS AND DISCUSSION

This part of our study is devoted to the investigation of magnetic ordering temperature T_m and transition temperature T_c'. For this purpose we have studied a model Hamiltonian which contains interactions involving scattering of Cooper pairs by localized 4f spins. In the first part, the reduced transition temperature, T_c' has been evaluated numerically as a function of impurity concentration. The reduced energy gap parameter is also expressed as a function of the new transition temperature analytically, and also comparisons with BCS type will be carried out graphically. In the second section the ordering temperature T_m against concentration will be manipulated numerically and plotted to discuss superconducing properties. We have used constants and experimental values from [23], [46], and [47] for calculations under this chapter.

4.1 T_c versus Concentration (n)

It is clear from AG [7] theory of pair-breaking that T_c is suppressed as the function of the impurity concentration, even though they have addressed uncorrelated spins. Kebede et al. [23] have also studied experimentally the variation of T_c with correlated doped impurities producing magnetic order. Even though Pr shows unusual properties

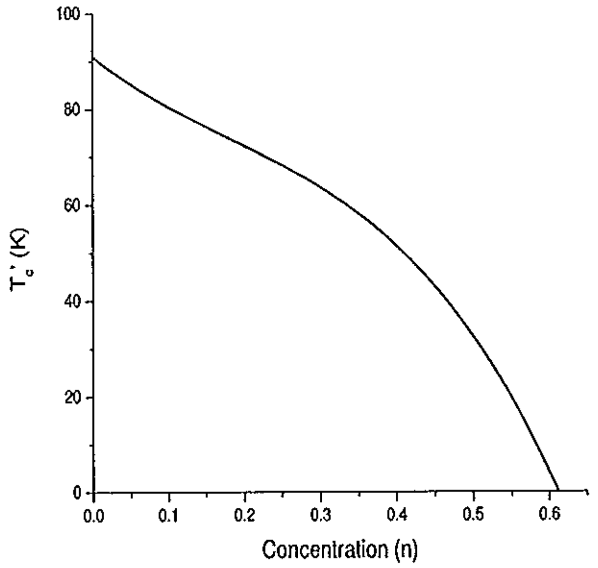

Figure 4.1: T_c' versus impurity concentration.

from compound to compound because of its mixed valance, magnetic moment etc., we have gone through its effect on YBCO system by producing magnetic ordering to a range of magnetic transition temperature. So we have taken the magnitude of spin, $S = 0.5$ for Pr^{+4} case. But if we use S=1 for Pr^{+3} case, the variation is more drastic. Therefore we have calculated the new transition temperature T_c' as $\Delta \rightarrow 0$ from Eq. (3.1.34) numerically when magnetic impurity is added, and the graph for different values of concentration is shown in Fig. 4.1. It is clearly seen from the graph that transition temperature is reduced as the Pr concentration increase because electrons get scattered and spin flipped.

Let us consider the following two equations as

$$1 = \lambda \int_0^{\hbar\omega_b} d\varepsilon_k \frac{\tanh \beta/2\sqrt{\varepsilon_k^2 + \Delta^2}}{\sqrt{\varepsilon_k^2 + \Delta^2}}, \tag{4.1.1}$$

$$1 = \lambda \int_0^{\hbar\omega_b} d\varepsilon_k \frac{\tanh \beta/2\sqrt{\varepsilon_k^2 + \Delta'^2}}{\sqrt{\varepsilon_k^2 + \Delta'^2}}. \tag{4.1.2}$$

If no magnetic impurity is added to the system, Eq. (4.1.2) goes to the celebrated BCS type expression, i.e., it reduces to Eq. (4.1.1). On the other hand, since energy gap is a measure of transition temperature, we also determined the modified gap parameter in relation with the new transition temperature analytically and we have taken the impurity concentration for instance, 0.2 for the determination of particular T_c'. Hence the ratio $\frac{\Delta(T)}{\Delta(0)}$ is a universal function of $\frac{k_BT}{\Delta(0)}$ or of $\frac{T}{T_c}$. In practice from Eq. (4.1.1), the values $\frac{\Delta(T)}{\Delta(0)}$ are given by the relation [46],

$$\frac{\Delta(T)}{\Delta(0)} = \tanh\left[\frac{T_c\Delta(T)}{T\Delta(0)}\right]. \tag{4.1.3}$$

Since Eqs. (4.1.1) and (4.1.2) have the same form, we can approximate Eq. (4.1.2) analytically by

$$\frac{\Delta'(T)}{\Delta'(0)} = \tanh\left[\frac{T_c'\Delta'(T)}{T\Delta'(0)}\right]. \tag{4.1.4}$$

Therefore, Figs. 4.2 and 4.3 show the variation of gap parameter with temperature with out the added magnetic impurity (the BCS type) and added impurity (the modified gap parameter) respectively. The shape of the two graphs are roughly similar, except showing different peak shapes, the latter one is reduced in the presence of magnetic impurity. That means, the suprconducting region is reduced drastically by the spin fluctuations, which weaken the BCS coupling depend on the Fermi wave number. This is because the spin fluctuations prefer the spin-triplet state of conduction electrons rather than the spin-singlet in a Cooper pair.

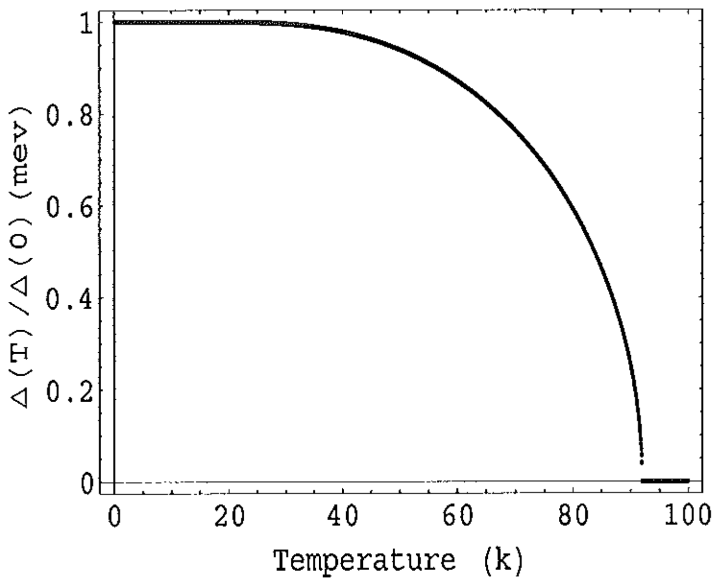

Figure 4.2: Gap parameter versus temperature with out impurity.

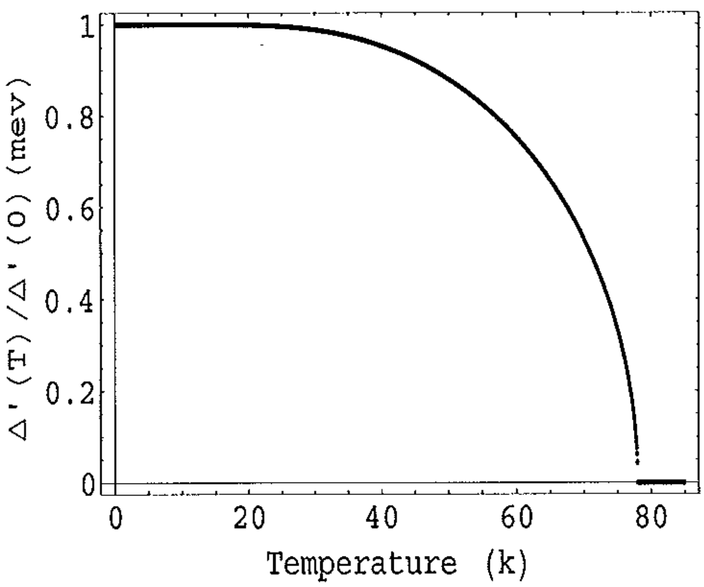

Figure 4.3: Gap parameter versus temperature in the presence of impurity.

Abrikosov and Gorkov [7] showed that at sufficiently high concentration of paramagnetic impurity, superconductivity is destroyed completely. In their theory T_c variation as a function of concentration is given by

$$\ln\frac{T_c}{T_{c0}} = \psi(0.5) - \psi(0.5 + \frac{n}{2\pi T_c}). \tag{4.1.5}$$

If we compare our graph Fig. 4.1 with that of Abrikosov-Gorkov pair-braking theory [48] and Kebede et al. [23] shown in Figs. 4.4 and 4.5 respectively, our's is less smooth, because the correlated spins produce an order which causes deviation from the smooth curve.

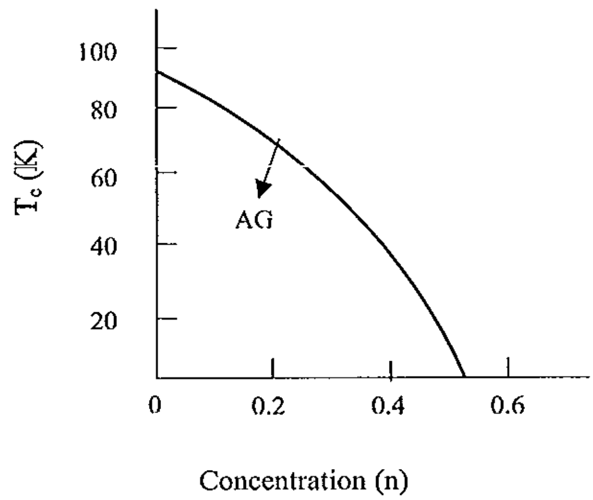

Figure 4.4: Superconducting transition temperature T_c Vs. Pr concentration in $Y_{1-x}Pr_xBa_2Cu_3O_{7-\delta}$ (AG theory).

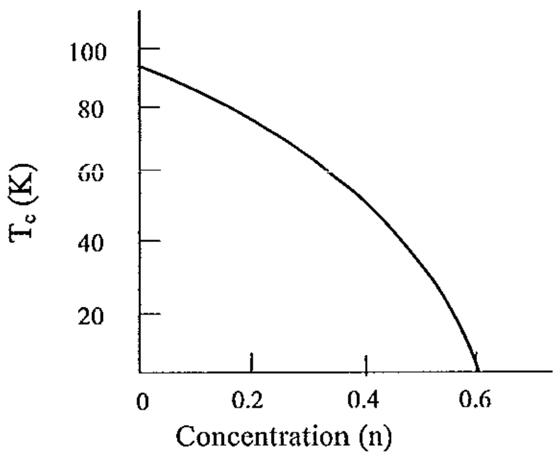

Figure 4.5: Superconducting transition temperature T_c Vs. Pr concentration in $Y_{1-x}Pr_xBa_2Cu_3O_{7-\delta}$ (Kebede et al. experiment).

4.2 T_m versus Concentration (n)

The origin of magnetic order resulting in destruction of superconductivity is due to quantum-mechanical interaction between the spins of the electrons and the atomic magnetic moments of Pr element. Below the superconducting transition temperature this exchange interaction attempts to align the Cooper pairs, and therefore exchange interaction places stringent limits on the existence of superconductivity. For ferromagnetic coupling χ increases asymptotically as the temperature is lowered and has maximum value at T_c [47]. Since magnetic susceptibility is a measure of magnetic ordering, we have taken its maximum value for our calculation in this section which is given experimentally [47]. Using Eq. (3.2.23) we have carried out the variation of magnetic ordering temperature for different values of concentration, and plotted in Fig. 4.6. From this graph we can see clearly that, as the impurity concentration is increased to a certain critical value, the ordering temperature T_m is increased which possibly reduces the superconducting region. By merging the two graphs (Figs. 4.1 and 4.6), we have got a region in which both superconductivity and ferromagnetism coexist as shown in Fig. 4.7. This phenomenon is clearly verified experimentally by Kebede et al. [23]. Thus, our prediction has got a good qualitative agreement with experiment.

Generally to say, Pr has unique properties and has a number of effects:- it changes the number of electrons, it alters the density of states, it scatters and flips the electrons so changing the Bloch states. Pr spins made themselves ordered via conduction electrons, and produce ferromagnetic ordering even though they are localized. Such type of ordering enhances suppression of superconductivity more than spin glass and antiferrromagnetic ordering [19]. The spin glass and antiferrromagnetic ordering are also harmful because they have an effect on shifting energy bands of the electrons/holes forming the Cooper pairs [19].

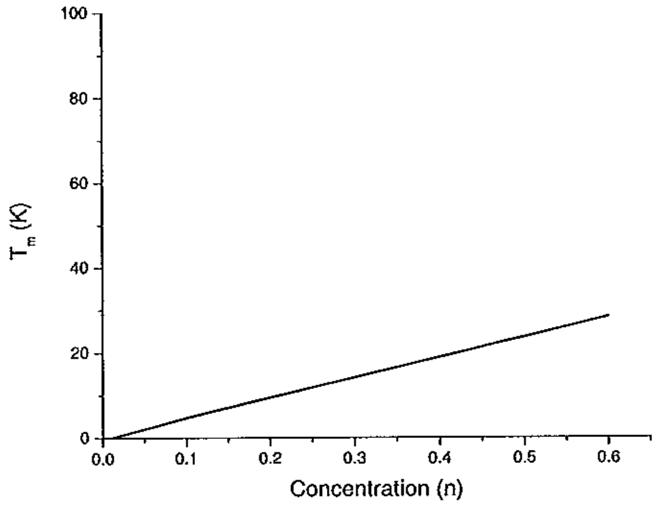

Figure 4.6: T_m versus impurity concentration.

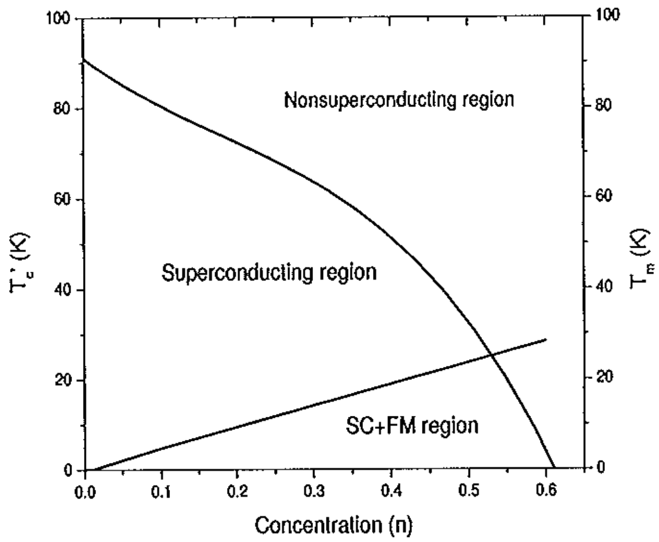

Figure 4.7: Co-existence of Superconductivity and Ferromagnetism.

Chapter 5

SUMMARY AND CONCLUSION

In the present investigation we have studied the effect of magnetic impurity on superconducting transition temperature T_c and the magnetic ordering temperature T_m. In the introduction part, we have seen high temperature superconductors with high T_c are progressively invented with the corresponding years. Low T_c superconductors also studied in this part. Chapter one is devoted to the brief introduction of superconductivity in general, and review of previous work, which has been carried out in recent years and also related to our investigation. In chapter two, we have had a brief account about double-time temperature dependent Green's function formalism of Quantum field theory. Under chapter three, we devoted the effect of Pr impurity on the system and constructed a model Hamiltonian on the frame work of BCS theory. In the first section of this chapter, we have formulated equation of motion which describes both the gap parameter (Δ) and T_c, and how they got depressed as the concentration of Pr impurity increased. In the second section a quantitative expression is given for magnetic ordering temperature (T_m) as a function of Pr concentration.

As we discussed in chapter four, with the range of impurity concentration just before the destruction of superconductivity, transition temperature is decreased. But the system has a finite density of states with zero excitation energy yet the system possesses an infinite conductivity. Therefore we conclude that energy gap is not sufficient parameter for superconductivity, an impurity spin acts as a Cooper pair-breaker and suppresser, and the ferromagnetic type ordering enhance the pair-breaking effect. More refined experiments will be required to study the interplay of superconductivity and magnetic order and their possible coexistence theoretically.

[31] L .P. Gokov and A. I. Rusinov, Sov. Phys. JETP **19**, 922(1961).

[32] K. H. Bennemann, Phys. Rev. Lett. **17**, 438(1966).

[33] F. Reif and M. A. Woolf, Phys. Rev. Lett. **9**, 315(1962).

[34] P. R. Weiss et al., Phys. Rev. **136**, A1500(1964).

[35] K. N. Yang et al., App. Phys. A **46**, 229(1988).

[36] G. Y. Gou and W. Temmermann, Phys. Rev. B **41**, 6372(1990).

[37] A. Matsuda et al., Phys. Rev. B **38**, 2910(1988).

[38] S. Ghamaty, Phys. Rev. B **43**, 5430(1990).

[39] J. J Neumeier et al., Phys. Rev. Lett. B **63**, 2516(1989).

[40] J. J Neumeier et al., Physica C **166**, 191(1996).

[41] J. Fink et al., Phys. Rev. B **42**, 4823(1990).

[42] S. Horn et al., Phys. Rev. B **36**, 389(1987).

[43] L. Seaman, Phys. Rev. B **42**, 6801(1990).

[44] K. Yosida, Phys. Rev. **106**, 893(1957).

[45] T. V. Ramakrishnan and C. M. Varma, Phys. Rev. B **24**, 137(1981).

[46] G. Rickayzen, Theory of Superconductivity, by John Wiley and Sons, Interscince, New York, 1965.

[47] O. Kahn, Molecular Magnetism; VCH: New York, 1993.

[48] M. B. Maple, Journal of Superconductivity **7**, 98(1994).